Essential contribution of CCL3 to alkali-induced corneal neovascularization by regulating vascular endothelial growth factor production by macrophages

Essential contribution of CCL3 to alkali-induced corneal neovascularization by regulating vascular endothelial growth factor production by macrophages

Peirong Lu,[1, 2, 3, 4] Longbiao Li,[2] Yu Wu,[4] Naofumi Mukaida,[4] and Xueguang Zhang[1,3]

[1]Clinical Immunology Key Laboratory of Jiangsu Province, [2]Department of Ophthalmology, the First Affiliated Hospital of Soochow University, China PR; [3]Biotechnology Institute, Soochow University, Suzhou, China PR; and [4]Division of Molecular Bioregulation, Cancer Research Institute, Kanazawa University, Japan

Running Title: CCL3 in Corneal Neovascularization

Key Words: chemokine; chemokine receptor; corneal injury; neovascularization; macrophage

Correspondence: Naofumi Mukaida, MD & PhD, Division of Molecular Bioregulation, Cancer Research Institute, Kanazawa University, 13-1 Takara-machi, Kanazawa 920-0934, Japan, Tel: +81-76-265-2768, E-mail: naofumim@kenroku.kanazawa-u.ac.jp or Xueguang Zhang, MD & PhD, Clinical Immunology Key Laboratory of Jiangsu Province, Soochow University, 188 Shizi Street, Suzhou 215006, China PR. E-mail: smbxuegz@public1.sz.js.cn

Abstract

Purpose: To evaluate the roles of CCL3, and its specific chemokine receptors, CCR1 and CCR5, in alkali-induced corneal neovascularization (CNV).

Methods: Wild-type (WT) BALB/c mice and CCL3-, CCR1- and CCR5-deficienct (KO) counterparts were underwent chemical denudation of corneal and limbal epithelium. CNV at 2 weeks after injury was quantified by immunostaining with anti-CD31. The angiogenic factor expression and the leukocyte accumulation at the early phase after injury were quantified by RT-PCR and immunohistochemical analysis, respectively.

Results: Alkali injury augmented the intraocular mRNA expression of CCL3 and its receptor, CCR1 and CCR5, together with a transient infiltration of F4/80-positive macrophages and Gr-1-positive neutrophils. Compared with WT mice, CCL3- and CCR5- but not CCR1-KO mice exhibited reduced CNV 2 weeks after injury, macroscopically and microscopically as evidenced by CD31-positive areas. Concomitantly, the infiltration of F4/80-positive macrophages but not Gr-1-positive neutrophils was significantly attenuated in CCL3 KO mice compared with WT mice. Intracorneal infiltration of CCR5 expressing cells was significantly impaired in CCL3 KO mice compared with WT mice. Alkali injury induced a massive increase in the intraocular mRNA expression of a potent angiogenic factor, vascular endothelial growth factor (VEGF) in WT mice and the increments were severely retarded in CCL3 KO mice. Moreover, CCL3 enhanced VEGF expression by murine peritoneal macrophages at mRNA and protein levels. Furthermore, topical CCL3 application reversed CNV, which was macroscopically and microscopically reduced in CCL3 KO mice at 2 weeks, to similar levels found in WT mice.

Conclusions: In alkali-induced CNV, CCL3 induced macrophages to infiltrate and produce VEGF by binding to CCR5 but not CCR1, and eventually promoted angiogenesis.

INTRODUCTION

Cornea is characterized by the absence of blood vessels under physiological conditions [1]. Corneal avascularity is maintained by the balance between angiogenic and anti-angiogenic molecules [2-6], and is required for optical clarity and maintenance of vision. Thus, corneal neovascularization (CNV) can lead to impaired vision when it arises from any causes including corneal infections, misuse of contact lens, chemical burn, and inflammation [7-9]. In most of these conditions, preceding the onset of CNV, a large number of neutrophils infiltrate into cornea followed by the infiltration of monocytes/macrophages. Although neutrophils are presumed to be involved in CNV, we previously proved that alkali-induced CNV developed independently of granulocyte infiltration [10].

Leukocyte infiltration is regulated by coordinative actions of adhesion molecules and chemokines [11]. The chemokine receptor expression pattern on leukocytes determines their responsiveness to each chemokine [11]. Monocytes/macrophages express a distinct set of chemokine receptors such as CCR1, CCR2, CCR5 and CX3CR1 on their cell surface [12-14]. We previously found a potent angiogenic factor, VEGF, was detected in intraocularly infiltrating monocytes/macrophages before CNV development [10]. Consistently, genetic ablation of either CCR2 or CCR5 gene markedly attenuated CNV [15,16], together with reduced intraocular VEGF production. In contrast, several groups provided evidence to indicate the anti-angiogenic activities of infiltrating macrophages in choroidal neovascularization [17]. In line with this notion, we also observed that intraocularly infiltrated CX3CR1-positive macrophages expressed anti-angiogenic molecules such as thrombospondins and were protective for alkali-induced CNV [18]. Thus, monocytes/macrophage population may be heterogeneous in terms of angiogenic activities, depending on their chemokine receptor expression pattern.

We previously observed that CCR1 was expressed on endothelial cells in human hepatoma tissue [19]. Furthermore, both CCR1 KO and CCL3 KO mice exhibited impairment in

carcinogen-induced hepatocarcinogenesis with reduced macrophage infiltration and intra-tumor neovascularization [20]. These observations would imply the essential involvement of the CCL3-CCR1 axis in neovascularization. Because CCL3, can also bind to CCR5 as well as CCR1 [21], we compared the molecular pathological changes in a frequently used ocular neovascularization model, alkali-induced CNV [10,15,16,18] between WT mice and mice deficient in CCL3, CCR1 or CCR5, in order to address the roles of CCL3 and its receptors in CNV. We provided the definitive evidence to indicate the involvement of the CCL3/CCR5 but not the CCL3/CCR1 axis in alkali-induced CNV.

MATERIALS AND METHODS

Reagents and antibodies: Recombinant CCL3/MIP-1α (270-LD) and goat anti-mouse CCL3 antibodies were obtained from R&D Systems (Minneapolis, MN). Rat anti-mouse F4/80 (clone A3-1) monoclonal antibody (mAb) was from Serotec (Oxford, United Kingdom). Rabbit polyclonal to CD31 (ab28364) was purchased from Abcam (Cambridge, UK). Rat anti-mouse CD31 (MEC13.3), purified rat anti-mouse-Ly-6G and Ly-6C (Gr-1) mAbs (clone RB6-8C5) and purified rat anti-mouse CCR5 mAb (clone C34-3448) were from BD Pharmingen (San Diego, CA). Goat anti-CCR1 pAb (C-20) was obtained from Santa Cruz Biotechnology (Santa Cruz, CA). Alexa Fluor (AF) 488 donkey anti-rat IgG (H+L), AF594 donkey anti-rabbit IgG (H+L) as well as AF594 donkey anti-goat IgG (H+L) were purchased from Invitrogen (Shanghai, China).

Mice: CCL3-deficient (CCL3 KO) mice were obtained from Jackson Laboratories (Bar Harbor, ME). CCR1-deficient (CCR1 KO) and CCR5-deficient (CCR5 KO) mice were generous gifts from Drs. P.M. Murphy and J.-L. Gao (NIADID, NIH, Bethesda, MD) [22], and from Dr. Kouji Matsushima (University of Tokyo, Tokyo, Japan), respectively [23]. These deficient mice were backcrossed with BALB/c for more than 8 generations. Pathogen-free BALB/c mice were obtained from Clea Japan (Yokohama, Japan) and were designated as WT mice. All animal experiments were performed under specific pathogen-free conditions in Institute for Experimental Animals, Kanazawa University, in accordance with the ARVO Statement for the Use of Animals in Ophthalmic and Vision Research and were complied with the standards set out in the Guidelines for the Care and Use of Laboratory Animals of Kanazawa University.

Alkali-induced corneal injury model: Corneal injury was induced by placing a 2-mm filter disc saturated with 1N NaOH onto the left eye of the mouse as previously described [10,18]. In some experiments, the alkali-treated eyes received 5 μl of CCL3 preparation dissolved in 0.2% sodium hyaluronate (Sigma-Aldrich, St. Louis, MO) at a concentration of 3 μg/ml or vehicle twice a day for 7 days immediately after the alkali injury. At the indicated time intervals, mice were killed, and whole eyes were removed. The eyes were fixed in 10% neutrally buffered

formalin or were snap frozen in OCT compound. In some mice, the corneas were removed from both eyes, were placed immediately into RNALate (Qiagen, Tokyo, Japan), and were kept at -86°C until total RNA extraction. Each experiment was repeated at least three times.

Biomicroscopic examination: Eyes were examined under a surgical microsystem (Lecia MZ16, Germany) 14 days after alkali injury by two independent observers without a prior knowledge of the experimental procedures, as described previously [10,18].

Histological and immunohistochemical analysis: The paraffin-embedded tissues were cut into 5-μm thick slices and were then subjected to hematoxylin and eosin staining. Other sections were deparaffinized with xylene and rehydrated through graded concentrations of ethanol for immunohistochemical detection of F4/80-, CCL3- , CCR1- or CCR5- positive cells as described previously [20]. The numbers of F4/80-positive cells were counted on 5 randomly chosen fields of corneal sections in each animal at 200-fold magnification [18,20], by an examiner without any prior knowledge of the experimental procedures. The numbers of positive cells per mm^2 were calculated.

A double-color immunofluorescence analysis: A double-color immunofluorescence analysis was performed to determine the cells expressing CCR5 and CCR2. Briefly, the fixed cryosections (8 μm thick) were incubated with PBS containing 1% normal donkey serum and 1% BSA to reduce nonspecific reactions. Thereafter, the sections were incubated with the combinations of rat anti-CCR5 and rabbit anti-CCR2 overnight at 4°C. After being rinsed with PBS, the sections were then incubated with the combination of Alexa Fluor 488 donkey anti-rat IgG and Alexa Fluor 594 donkey anti-rabbit IgG (1/100) for 40 min at room temperature in the dark. Finally, the sections were washed with PBS and immunofluorescence was visualized in a dual-channel mode on a fluorescence microscope (Olympus, Tokyo, Japan). Images were processed using Adobe Photoshop software version 7.0.

Enumeration of corneal neovascularization: The deparaffinized sections (5 μm thick) and

the fixed cryosections (8 μm thick) were stained using rabbit anti-CD31 (ab28364) [10] and rat anti-CD31 antibody (MEC13.3) [18], respectively. The numbers and sizes of the CNV were determined as described previously [10], by an examiner with no knowledge of the experimental procedures. Most sections were from the central region of the cornea. The numbers and areas of corneal neovascularization were evaluated on at least two sections from each eye.

Semi-quantitative reverse transcription (RT)-polymerase chain reaction (PCR): Total RNAs were extracted from the corneas or cultured macrophages with the use of RNeasy Mini Kit (Qiagen, Tokyo, Japan) and the resultant RNA preparations were further treated with ribonuclease-free deoxyribonuclease (DNase) I (Life Technologies Inc., Gaithersburg, MD) to remove genomic DNA. Two μg of total RNA were reverse-transcribed at 42°C for 1 hour in 20 μl of reaction mixture containing mouse Moloney leukemia virus reverse transcriptase and hexanucleotide random primers (Qiagen). Serially two-fold diluted cDNA was amplified for β-actin (Table 1) to estimate the amount of transcribed cDNA. Then, equal amounts of cDNA products were amplified for the target genes using the primers under the following condition consisting of denaturation at 94°C for 2 min, followed by the optimal cycles of 30 sec at 94°C, 45 sec at 53-57°C, 1 min at 72°C, and a final 10 min extension step at 72°C (Table 1). The amplified PCR products were fractionated on a 1.0% agarose gel and visualized by ethidium bromide staining. The band intensities were measured and the ratios to β-actin were determined with the aid of NIH Image Analysis software.

Murine peritoneal macrophages isolation and culture: Peritoneal macrophages were obtained as described previously [18]. The cells were suspended in antibiotic-free RPMI medium containing 10% fetal bovine serum (FBS), and incubated in a humidified incubator at 37°C in 5% CO_2 in 24-well cell culture plates (Nalge Nunc International Corp., Naperville, IL). Two hours later, non-adherent cells were removed, and the medium was replaced. The cells were then stimulated with the indicated concentrations of murine CCL3 for 12 hours. Total RNAs were extracted from the cultured cells and subjected to RT-PCR as described above. In another series of experiments, murine macrophages were seeded onto the 12-well-plates at 5×10^5 cells/well. After adhesion, the cells were stimulated with the indicated concentrations of murine CCL3 for

24 hours in a 37°C incubator with 5% CO_2. Supernatants were collected to determine VEGF concentrations by using Mouse VEGF ELISA Kit (R&D Systems, Minneapolis, MN) according to the manufacturer's instructions.

Statistical analysis: The means and standard error of the mean (SEM) were calculated on all parameters determined in the study. Data were analyzed statistically using one-way analysis of variance (ANOVA) or two-tailed Student's *t* test. A value of $p < 0.05$ was accepted as statistically significant.

RESULTS

Intracorneal expression of CCL3 and its receptor, CCR1 and CCR5, after alkali-induced corneal injury: We first examined the expression of CCL3, a ligand for CCR5 and CCR1, in corneas after alkali-induced injury. CCL3 mRNA was barely detected in untreated eyes and was markedly increased after alkali injury (Figure 1A). Concomitantly, CCL3 protein was immunohistochemically detected in epithelial cells and infiltrating cells after alkali injury, but not in untreated eyes (Figure 1B). Moreover, alkali injury markedly augmented the mRNA expression of specific receptors for CCL3, CCR1 and CCR5 (Figure 1A). Furthermore, immunohistochemical analysis demonstrated the infiltration of CCR1-expressing leukocytes, starting 2 days after the injury and increasing thereafter (Figure 1B). These observations suggest that alkali injury induced intracorneal production of CCL3, which in turn attracted CCR1- or CCR5-expressing leukocytes into cornea.

Impaired alkali-induced CNV in CCL3, CCR5 KO but not CCR1 KO mice: We next explored the effects of genetic ablation of CCL3, CCR1, and CCR5 on alkali-induced CNV. CNV was macroscopically evident in WT mice, 2 weeks after the injury, as we previously reported [10]. In line with the previous report [16], macroscopic CNV was markedly attenuated in CCR5 KO mice (Figure 2A). Moreover, macroscopic CNV was markedly reduced in CCL3 KO but not CCR1 KO mice (Figures 2A,B,C). Although corneas are physiologically avascular, alkali injury markedly increased the vascular areas in corneas in WT and CCR1 KO mice to similar extents but the increment was significantly reduced in CCL3 KO mice (Figures 2B,C). These observations would indicate that the CCL3-CCR5 but not the CCL3-CCR1 axis was indispensable for alkali-induced CNV.

Reduced intraocular macrophage infiltration in CCL3 but not CCR1 KO mice: We previously observed that Gr-1-positive granulocytes and F4/80-positive macrophages infiltrated injured cornea, reaching their peak levels 2 to 4 days after the injury in WT mice [10,18]. Leukocytes, particularly monocytes/macrophages, can be a rich source of angiogenic factors [24-28]. Given the fact that CCL3 recruit macrophages which express CCR1 and CCR5, we

examined the effects of CCL3 deficiency on leukocyte infiltration into wounded cornea. Neither F4/80-positive macrophages nor Gr-1-positive granulocytes were present in untreated corneas of WT and CCL3 KO mice. Gr-1-positive granulocytes infiltrated into cornea to similar extents in WT and CCL3 KO mice after the injury (data not shown). By contrast, F4/80-positive macrophage infiltration was markedly reduced in CCL3 KO but not in CCR1 KO mice, compared with WT mice (Figure 2D). Thus, CCL3 may regulate intraocular infiltration of F4/80-positive macrophages but not granulocytes.

Reduced VEGF expression in CCL3 KO mice after alkali injury: The balance between angiogenic and anti-angiogenic factors can determine the outcome of angiogenesis processes in various situations. Hence, we examined the mRNA expression of angiogenic and anti-angiogenic factors in corneas after the injury. Alkali injury increased intraocular mRNA expression of an angiogenic factor, bFGF, and an anti-angiogenic molecule, TSP-1, in WT and CCL3 KO mice to similar extents (Figure 3A). By contrast, the mRNA expression of another potent angiogenic factor, VEGF, was markedly augmented in WT mice and the increase was markedly attenuated in CCL3 KO mice (Figure 3A).

Enhanced VEGF expression by murine peritoneal macrophages with CCL3 stimulation: We next examined the effects of exogenous CCL3 on VEGF expression by mouse peritoneal macrophages at mRNA and protein levels. CCL3 enhanced markedly the mRNA expression of VEGF by peritoneal macrophages (Figure 3B). Concomitantly, CCL3 increased VEGF protein production by macrophages, in a dose-dependent manner (Figure 3C). These observations would indicate that CCL3 can activate macrophages to produce an angiogenic factor, VEGF.

Simultaneous CCR2 expression by intracorneally infiltrating CCR5-expressing cells: We previously revealed that the CCL2/CCR2 interactions could induce VEGF expression. Hence, we next examined whether intraocularly infiltraiting CCR5-expressing cells expressed CCR2. A double-color immunofluorescence analysis demonstrated that CCR5-expressing cells also expressed CCR2 (Figure 4A). Moreover, alkali injury-induced increases in intracorneal

CCR5-positive cell numbers were attenuated in CCL3 KO mice (Figures 4B, C). Thus, it is likely that CCL3 can regulate intraocular infiltration of CCR5-expressing macrophages, which can express VEGF by the CCL2/CCR interactions.

Restoration of alkali-induced CNV in CCL3 KO mice by topical CCL3 application: Finally we examined the effects of topical CCL3 application on alkali-induced CNV of CCL3 KO mice. CCL3 KO mice exhibited reduced alkali-induced CNV at both a macroscopic and microscopic level, compared with WT mice (Figures 5A to C). Topical CCL3 application reversed CNV to a similar extent to WT mice (Figures 5A to C). Concomitantly, CCL3 treatment reversed the macrophage infiltration in CCL3 KO mice to similar levels as WT mice (Figure 5D). Thus, CCL3 may induce the infiltration of macrophages, which in turn may produce a potent angiogenic factor, VEGF, and eventually promote alkali-induced CNV.

DISCUSSION

Tissue injury induced the expression of various growth factors, cytokines, and chemokines, which contribute to tissue repair in a coordinated manner [29]. In cooperation with adhesion molecules, chemokines can regulate the trafficking of various types of leukocytes, which in turn regulate two processes of tissue repair, granulation tissue formation and neovasularization, by producing various growth factors and cytokines [29-32]. Moreover, several chemokines can directly regulate neovascularization [33]. Alkali injury induced a transient macrophage infiltration into eyes with enhanced intraocular CCL3 expression. Several independent groups reported that CCL3 has direct effects on endothelial cells [33] and that its receptor, CCR1, was expressed on certain types of endothelial cells [19,20]. However, CCL3 can restore CNV in CCL3 KO mice to similar levels shown by WT mice. This restoration of CNV is seen even if CCL3 was administered only in the early phase after the injury, at the time when the endothelial cells are absent. Thus, CCL3 may not directly target endothelial cells in this model.

Cornea lacks any vasculature under physiological conditions. Corneal avascularity is maintained by the balance between angiogenic factors including VEGF and bFGF, and anti-angiogenic factors including TSP-1 and soluble VEGF receptor I [1,2]. Alkali injury augmented intraocular mRNA expression of bFGF and TSP-1 in CCL3 KO mice to an extent similar to WT mice. On the contrary, alkali-induced enhanced VEGF expression was markedly attenuated in CCL3 KO mice. Because soluble VEGF receptor I, a decoy receptor for VEGF, is constitutively present and acts as a major anti-angiogenic factor in cornea [1], the reduced VEGF expression in CCL3 KO mice may account for attenuated CNV after alkali injury in these mice. Moreover, CCL3 can augment VEGF production by macrophages. Thus, it is likely that CCL3 induced CNV indirectly by inducing the infiltration and activation of macrophages, a major source of VEGF.

The crucial roles of macrophages in tissue repair are proposed based on the observations that these cells can produce abundantly various growth and angiogenic factors. Similar to other types of leukocytes, macrophage infiltration is regulated mainly by coordinate actions of adhesion molecules and chemokines. Chemokines bind to their cognate receptor on leukocytes and exert their actions. Macrophages express a limited set of chemokine receptors including CCR1, CCR2, CCR5, and CX3CR1 and exhibit chemotaxis to their ligands [12-14]. CCL3 utilizes two distinct receptors, CCR1 and CCR5 [12], with slight differences in their expression patterns [12,21]. Reduced CNV in CCR5 KO mice prompted us to evaluate the roles of CCL3 and CCR1 in this model. CCL3 deficiency but not CCR1 deficiency reduced alkali-induced CNV. We recently observed that bleomycin-induced intrapulmonary macrophage accumulation and subsequent pulmonary fibrosis was attenuated in CCL3 KO and CCR5 KO, but not CCR1 KO mice [34]. These observations suggest that CCR5-expressing cells were distinct from CCR1-expressing cells. Indeed, a double-color immunofluorescence analysis demonstrated that CCR5-expressing cells did not express CCR1 simultaneously (our unpublished data). Thus, CCL3 may generally regulate macrophage functions by binding CCR5 but not CCR1 expressed on their surface.

A partial reduction of macrophage infiltration by CCL3 deficiency suggests the contribution of other chemokines such as CCL2 and CX3CL1 to macrophage infiltration. This may further suggest the heterogeneity of monocytes/macrophages in terms of chemokine receptor expression pattern, as previously suggested by Geissmann and colleagues who proposed the presence of two blood monocytes, inflammatory $CX3CR1^{low}CCR2^{+}$ and resting $CX3CR1^{high}CCR2^{-}$ populations [35]. Macrophages are presumed to exert pro-angiogenic actions under various situations [24-28] but Apte and colleagues demonstrated anti-angiogenic activities of macrophages in CNV [17]. These observations suggest the functional heterogeneity among macrophages during angiogenesis process. Indeed, we demonstrated that CX3CR1-positive macrophages could dampen alkali-induced CNV by producing anti-angiogenic molecules [18], in contrast to the

observations on CCR2-deficient mice [15]. We previously revealed that the CCL2/CCR2 interactions were involved in VEGF production [18] and here observed that CCR5-expressing cells expressed simultaneously CCR2. Thus, CCR5 deletion reduced the number of CCR2-expressing macrophages, the cells that can express VEGF, and eventually prevented alkali-induced CNV.

Several independent groups reported the presence of resident macrophages, dendritic cells, langerhans cells and T cells in the normal corneas [36-39]. The numbers of resident macrophages in normal corneal stroma are around 100 per mm^2 [36] and we detected few, if any, F4/80- or CD68-positive macrophages in normal corneas in the current experimental condition [18]. Thus, it is not likely that corneal resident macrophages contribute directly to CNV in this model.

The simple dichotomy of monocytes/macrophages proposed by Geissmann was, however, complicated by the observation that $CCR2^-$ and $CCR2^+$ monocytes depended on CCR5 and CX3CR1, respectively, when they entered into atherosclerotic plaques [40]. Ambati and colleagues reported that CCR2 deficiency inhibited CNV but did not examine the roles of macrophages in this process [15]. Thus, it still remains unclear what the effects of the CCR2 axis on macrophage infiltration in CNV or the interaction between the CCR2 and CCR5 axis are. More detailed analysis on this point will clarify the molecular and cellular mechanisms underlying macrophage infiltration and subsequent CNV development.

ACKNOWLEDGEMENTS

This work was supported by International Cooperative Program of Kanazawa University (NM), and National Natural Science Foundation in China (NSFC No 30572120, NSFC No 30771978), Jiangsu Natural Science Foundation (BK2006528), China Postdoctoral Science Foundation (2005038587), and grants from Soochow University (PL), and National Natural Science Key Program Foundation in China (NSFC No 30330540) (XZ). We express our sincere gratitude to Dr Che John Connon, PhD (Division of Pharmacology, School of Pharmacy, University of Reading, UK) for creative reading.

Disclosures

The authors have no financial conflict of interest.

REFERENCES

1. Ambati BK, Nozaki M, Singh N, Takeda A, Jani PD, Suthar T, Albuquerque RJC, Richter E, Sakurai E, Newcomb MT, Kleinman ME, Caldwell RB, Lin Q, Ogura Y, Orecchia A, Samuelson DA, Agnew DW, St. Leger J, Green WR, Mahasreshti PJ, Curiel DT, Kwan D, Marsh H, Ikeda S, Leiper LJ, Collinson JM, Bogdanovich S, Khurana TS, Shibuya M, Baldwin ME, Ferrara N, Gerber H-P, DeFalco S, Witta J, Baffi JZ, Raisler BJ, Ambati J. Corneal avascularity is due to soluble VEGF receptor-1. Nature 2006;443:993-7.
2. Cursiefen C, Masli S, Ng TF, Dana MR, Bornstein P, Lawler J, Streilein JW. Roles of thrombospondin-1 and -2 in regulating corneal and iris angiogenesis. Invest Ophthalmol Vis Sci 2004;45:1117-24.
3. Gao G, Ma J. Tipping the balance for angiogenic disorders. Drug Discov Today 2002;7:171-2.
4. Zhang SX, Ma JX. Ocular neovascularization: Implication of endogenous angiogenic inhibitors and potential therapy. Prog Retin Eye Res 2007;26:1-37.
5. Edelman JL, Castro MR, Wen Y. Correlation of VEGF expression by leukocytes with the growth and regression of blood vessels in the rat cornea. Invest Ophthalmol Vis Sci 1999;40:1112-23.
6. Lai CM, Spilsbury K, Brankov M, Zaknich T, Rakoczy PE. Inhibition of corneal neovascularization by recombinant adenovirus mediated antisense VEGF RNA. Exp Eye Res 2002;75:625-34.
7. Chang JH, Gabison EE, Kato T, Azar DT. Corneal neovascularization. Curr Opin Ophthalmol 2001;12:242-9.
8. Epstein RJ, Stulting RD, Hendricks RL, Harris DM. Corneal neovascularization. Pathogenesis and inhibition. Cornea 1987;6:250-7.
9. Klintworth GK, Burger PC. Neovascularization of the cornea: current concepts of its pathogenesis. In Ophthalmol Clin 1983;23:27-39.
10. Lu P, Li L, Mukaida N, Zhang X. Alkali-induced corneal neovascularization is independent of CXCR2-mediated neutrophil infiltration. Cornea 2007;26:199-206.
11. Taub DD. Chemokine-leukocyte interactions. The voodoo that they do so well. Cytokine

Growth Factor Rev 1996;7:355-76.

12. Le Y, Zhou Y, Iribarren P, Wang J. Chemokines and chemokine receptors: their manifold roles in homeostasis and disease. Cell Mol Immunol 2004;1:95-104.
13. Barlic J, Zhang Y, Foley JF, Murphy PM. Oxidized lipid-driven chemokine receptor switch, CCR2 to CX3CR1, mediates adhesion of human macrophages to coronary artery smooth muscle cells through a peroxisome proliferator-activated receptor gamma-dependent pathway. Circulation 2006;114:807-19.
14. Imaizumi T, Yoshida H, Satoh K. Regulation of CX3CL1/fractalkine expression in endothelial cells. J Atheroscler Thromb 2004;11:15-21.
15. Ambati BK, Joussen AM, Kuziel WA, Adamis AP, Ambati J. Inhibition of corneal neovascularization by genetic ablation of CCR2. Cornea 2003;22:465-7.
16. Ambati BK, Anand A, Joussen AW, Kuziel WA, Adamis AP, Ambati J. Sustained inhibition of corneal neovascularization by genetic ablation of CCR5. Invest Ophthalmol Vis Sci 2003;44:590-3.
17. Apte RS, Richter J, Herndon J, Ferguson TA. Macrophages inhibit neovascularization in a murine model of age-related macular degeneration. PLoS Med 2006;3:1371-81.
18. Lu P, Li L, Kuno K, Wu Y, Baba T, Li YY, Zhang X, Mukaida N. Protective roles of the fractalkine/CX3CL1-CX3CR1 axis against alkali-induced corneal neovascularization through enhanced anti-angiogenic factor expression. J Immunol 2008;108: 4283-91.
19. Lu P, Nakamoto Y, Nemoto-Sasaki Y, Wang H, Hashii M, Ohmoto Y, Kaneko S, Kobayashi K, Mukaida N. Potential interaction between CCR1 and its ligand, CCL3, induced by endogenously produced interleukin-1 in human hepatomas. Am J Pathol 2003;162:1249-58.
20. Yang X, Lu P, Fujii C, Nakamoto Y, Gao JL, Kaneko S, Murphy PM, Mukaida N. Essential contribution of a chemokine, CCL3, and its receptor, CCR1, to hepatocellular carcinoma progression. Int J Cancer 2006;118:1869-76.
21. Zlotnik A, Yoshie O. Chemokines: A New Classification Review System and Their Role in Immunity. Immunity 2000;12:121-7.
22. Gao JL, Wynn TA, Chang Y, Lee EJ, Broxmeyer HE, Cooper S, Tiffany HL, Westphal H,

Kwon-Chung J, Murphy PM. Impaired host defense, hematopoiesis, granulomatous inflammation and type 1-type 2 cytokine balance in mice lacking CC chemokine receptor 1. J Exp Med 1997;185:1959-68.

23. Murai M, Yoneyama H, Ezaki T, Suematsu M, Terashima Y, Harada A, Hamada H, Asakura H, Ishikawa H, Matsushima K. Peyer's patch is the essential site in initiating murine acute and lethal graft-versus-host reaction. Nat Immunol 2003;4:154-60.
24. Sakurai E, Anand A, Ambati BK, van Rooijen N, Ambati J. Macrophage depletion inhibits experimental choroidal neovascularization. Invest Ophthalmol Vis Sci 2003;44:3578-85.
25. Grossniklaus HE, Ling JX, Wallace TM, Dithmar S, Lawson DH, Cohen C, Elner VM, Elner SG, Sternberg P Jr. Macrophage and retinal pigment epithelium expression of angiogenic cytokines in choroidal neovascularization. Mol Vis 2002;21:119-26.
26. Tsutsumi C, Sonoda KH, Egashira K, Qiao H, Hisatomi T, Nakao S, Ishibashi M, Charo IF, Sakamoto T, Murata T, Ishibashi T. The critical role of ocular-infiltrating macrophages in the development of choroidal neovascularization. J Leukocyte Biol 2003;74:25-32.
27. Espinosa-Heidmann DG, Suner IJ, Hernandez EP, Monroy D, Csaky KG, Cousins SW. Macrophage depletion diminishes lesion size and severity in experimental choroidal neovascularization. Invest Ophthalmol Vis Sci 2003;44:3586-92.
28. Oh H, Takagi H, Takagi C, Suzuma K, Otani A, Ishida K, Matsumura M, Ogura Y, Honda Y. The potential angiogenic role of macrophages in the formation of choroidal neovascular membranes. Invest Ophthalmol Vis Sci 1999;40:1891-8.
29. Gillitzer R, Goebeler M. Chemokines in cutaneous wound healing. J Leukoc Biol 2001;69:513-21.
30. Werner S, Grose R. Regulation of wound healing by growth factors and cytokines. Physiol Rev 2003;83:835-70.
31. Martin P, Leibovich SJ. Inflammatory cells during wound repair: the good, the bad and the ugly. Trends Cell Biol 2005;15:599-607.
32. Mori R, Kondo T, Ohshima T, Ishida Y, Mukaida N. Accelerated wound healing in tumor necrosis factor receptor p55-deficient mice with reduced leukocyte infiltration. FASEB J 2002;16:963-74.

33. Ryschich E, Lizdenis P, Ittrich C, Benner A, Stahl S, Hamann A, Schmidt J, Knolle P, Arnold B, Hämmerling GJ, Ganss R. Molecular fingerprinting and autocrine growth regulation of endothelial cells in a murine model of hepatocellular carcinoma. Cancer Res 2006;66:198-211.
34. Ishida Y, Kimura A, Kondo T, Hayashi T, Ueno M, Takakura N, Matsushima K, Mukaida N. Essential roles of the CC chemokine ligand 3-CC chemokine receptor 5 axis in bleomycin-induced pulmonary fibrosis through regulation of macrophage and fibrocyte infiltration. Am J Pathol 2007;170:843-54.
35. Geissmann F, Jung S, Littman DR. Blood monocytes consist of two principal subsets with distinct migratory properties. Immunity 2003;19:71-82.
36. Brissette-Storkus CS, Reynolds SM, Lepisto AJ, Hendricks RL. Identification of a novel macrophage population in the normal mouse corneal stroma. Invest Ophthalmol Vis Sci 2002;43:2264-71.
37. Hamrah P, Liu Y, Zhang Q, Dana MR. The corneal stroma is endowed with a significant number of resident dendritic cells. Invest Ophthalmol Vis Sci 2003;44:581-9.
38. Hamrah P, Zhang Q, Liu Y, Dana MR. Novel characterization of MHC class II-negative population of resident corneal Langerhans cell-type dendritic cells. Invest Ophthalmol Vis Sci 2002;43:639-46.
39. Mott KR, Osorio Y, Brown DJ, Morishige N, Wahlert A, Jester JV, Ghiasi H. The corneas of naive mice contain both CD4+ and CD8+ T cells. Mol Vis. 2007;13:1802-12.
40. Tacke F, Alvarez D, Kaplan TJ, Jakubzick C, Spanbroek R, Llodra J, Garin A, Liu J, Mack M, van Rooijen N, Lira SA, Habenicht AJ, Randolph GJ. Monocyte subsets differentially employ CCR2, CCR5, and CX3CR1 to accumulate within atherosclerotic plaques. J Clin Invest 2007;117:185-94.

Footnotes

[1]Clinical Immunology Key Laboratory of Jiangsu Province, [2]Department of Ophthalmology, the First Affiliated Hospital of Soochow University, China PR; [3]Biotechnology Institute, Soochow University, Suzhou, China PR; and [4]Division of Molecular Bioregulation, Cancer Research Institute, Kanazawa University, Japan

This work was supported by International Cooperative Program of Kanazawa University (to NM), National Natural Science Foundation in China (NSFC No 30572120, NSFC No 30771978), Jiangsu Natural Science Foundation (BK2006528), China Postdoctoral Science Foundation (2005038587), and grants from Soochow University (to PL), and National Natural Science Key Program Foundation in China (NSFC No 30330540) (to XZ).

Address correspondence to Naofumi Mukaida, MD & PhD, Division of Molecular Bioregulation, Cancer Research Institute, Kanazawa University, 13-1 Takara-machi, Kanazawa 920-0934, Japan, Tel: +81-76-265-2768, E-mail: naofumim@kenroku.kanazawa-u.ac.jp or Xueguang Zhang, MD & PhD, Clinical Immunology Key Laboratory of Jiangsu Province, Soochow University, 188 Shizi Street, Suzhou 215006, China PR. E-mail: smbxuegz@public1.sz.js.cn

Legends for Figures

Figure 1. The expression of CCL3 and its receptors in cornea after alkali injury. (A) Semi-quantitative RT-PCR was performed to assess mRNA expression of CCL3 and its receptors, CCR1 and CCR5 and the ratios of target gene expression to β-actin were determined. All values represent means ± SEM of 3 to 5 independent measurements. (B) Whole eyes were obtained at 0, 2, 4 and 7 days after alkali injury and processed to immunohistochemical analysis using anti-CCL3 (upper panels) or anti-CCR1 antibodies (lower panels). Representative results from 5 individual animals are shown here. Original magnifications, ×400. Scale bar, 50 μm.

Figure 2. Alkali-induced CNV and macrophage infiltration. (A) Macroscopic appearance of WT, CCL3 KO, CCR1 KO and CCR5 KO mouse eyes 2 weeks after alkali injury. Representative results from at least 10 animals in each group are shown here. (B) Corneal tissues were obtained at 2 weeks after the injury from WT, CCR1 KO, CCL3 KO mice. Tissues were stained with hematoxylin and eosin (left panels) or immunostained with anti-CD31 antibodies (right panels) and representative results from 5 individual animals are shown here. Original magnifications, ×400. Scale bar, 50 μm. (C) CNV numbers per mm^2 in hot spots and % CNV areas in hot spots were determined on corneas obtained from WT or KO mice 2 weeks after the injury, and are shown in upper and lower panels, respectively. Each value represents mean and SEM (n=5 animals). *, $p<0.05$, WT vs CCL3 KO mice. (D) The numbers of infiltrated F4/80-positive macrophages were determined at 2 and 4 days after the injury. Each value mean the mean and SEM (n=5). **, $p<0.01$, WT vs CCL3 KO mice.

Figure 3. (A) RT-PCR analysis of pro-angiogenic and anti-angiogenic gene expression in the injured corneas of WT and CCL3 KO mice. RT-PCR analysis was performed on total RNA's extracted from eyes at 0, 2, 4 and 7 days after alkali injury and the ratios of VEGF, bFGF, and TSP-1, to β-actin of WT (black bars) and CCL3 KO mice (open bars) were determined. All values represent means and SEM (n=3 to 5 animals). *, $p<0.05$; $^{\#}$, $p<0.01$, WT vs KO mice. (B and C) The effects of CCL3 on VEGF expression by murine peritoneal macrophages. (B)

RT-PCR was performed on macrophages incubated with the indicated concentrations of CCL3 for 12 hours and the ratios of VEGF to β-actin was calculated. Each value represents the mean and SEM (n=3). (C) Murine macrophages were stimulated with either 0, 10 or 100 ng/ml of CCL3 for 24 hours. VEGF concentrations in the supernatants were determined with ELISA as described in Materials and Methods. The representative results from three independent experiments are shown. *, $p<0.05$; **, $p<0.01$, compared to untreated.

Figure 4. (A) A double-color immunofluorescence analysis of CCR5-expressing cells. Corneas were obtained from WT mice 0 and 4 days after the injury. The samples were immunostained with the combination of anti-CCR5 and anti-CCR2 antibodies as described in Materials and Methods and observed under a fluorescence microscopy (original magnification, ×400). Signals were digitally merged in right panels. Arrows indicate the double-positively stained-cells. Representative results from three independent experiments are shown. (B) Corneal tissues from WT mice (left panel) or CCL3 KO mice (right panel) obtained 4 days after the injury were stained with anti-CCR5 Ab. Scale bar, 100μm. (C) The numbers of intracorneal CCR5-positive cells at 4 days after the injury were determined as described in Materials and Methods and the mean and SEM are shown here (n=5).

Figure 5. The effects of topical CCL3 application on CNV. (A) Macroscopic appearance of WT, CCL3 KO mice, or CCL3 KO mice topically applied with CCL3, at 2 weeks after alkali injury. Representative results from 5 animals in each group are shown here. (B) Corneal tissues were obtained 2 weeks after the injury from WT, CCL3 KO mice, or CCL3 KO mice topically applied with CCL3, and were immunostained with anti-CD31 antibodies. Representative results from 5 individual mice in each group are shown. Original magnification, ×400. Scale bar, 50 μm. (C) The CNV numbers per mm^2 in hot spots (left panel) and % CNV areas in hot spots (right panel) were determined. Each value represents mean and SEM (n=5 animals). *, $p<0.05$; **, $p<0.01$, compared with CCL3 KO. (D) The numbers of infiltrated F4/80-positive macrophages were determined on WT, CCL3 KO, or CCL3 KO treated with CCL3, at 2 days after the injury. Each value mean the mean and SEM (n=5). **, $p<0.01$, compared with CCL3 KO.

Figure 1 Lu et al

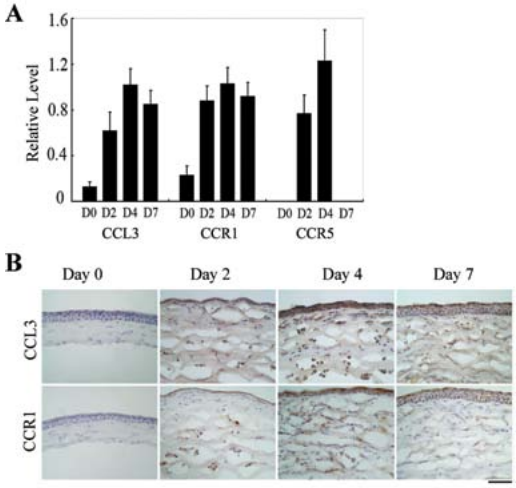

Figure 2 Lu et al

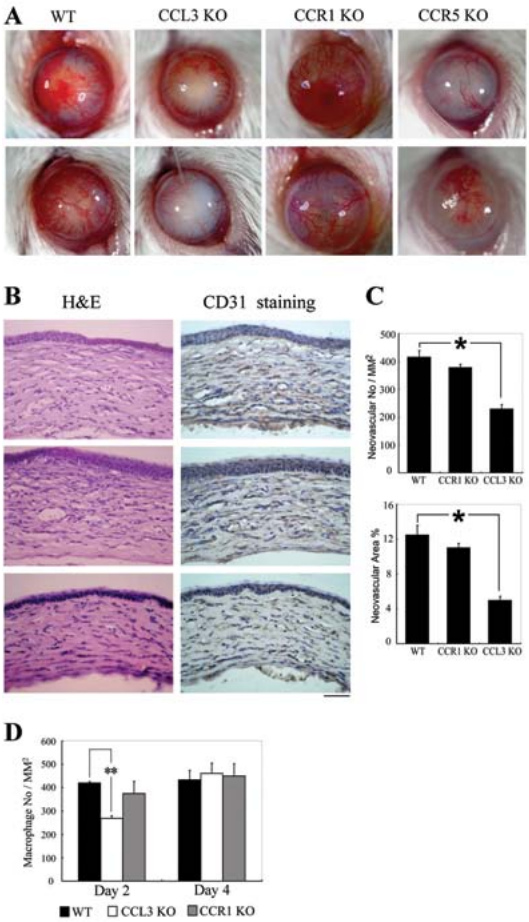

Figure 3 Lu et al

as Figure 4

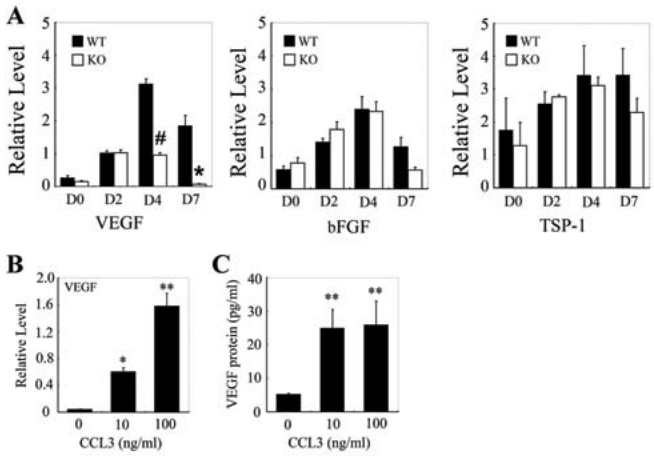

Figure 4 Lu et al

as Figure 5

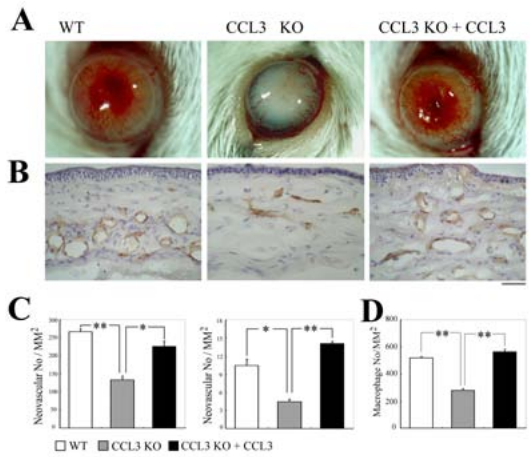

Figure 3 Lu et al